

UNCLASSIFIED

Copy 6  
RM L56L06

C.2



# RESEARCH MEMORANDUM

EXPLORATORY INVESTIGATION OF THE EFFECT OF WING SLOTS AND  
LEADING-EDGE SLATS ON THE LONGITUDINAL STABILITY  
CHARACTERISTICS OF A 45° SWEEPBACK  
WING-FUSELAGE CONFIGURATION

By Chris C. Critzos

Langley Aeronautical Laboratory  
Langley Field, Va.

CLASSIFICATION CHANGED  
UNCLASSIFIED

LIBRARY COPY

FEB 15 1957

LANGLEY AERONAUTICAL LABORATORY  
LIBRARY, NACA  
LANGLEY FIELD, VIRGINIA

CLASSIFIED DOCUMENT

This material contains information affecting the National Defense of the United States within the meaning of the espionage laws, Title 18, U.S.C., Secs. 793 and 794, the transmission or revelation of which in any manner to an unauthorized person is prohibited by law.

**NATIONAL ADVISORY COMMITTEE  
FOR AERONAUTICS**

WASHINGTON

February 8, 1957

NACA RM L56L06

~~CONFIDENTIAL~~



## NATIONAL ADVISORY COMMITTEE FOR AERONAUTICS

## RESEARCH MEMORANDUM

EXPLORATORY INVESTIGATION OF THE EFFECT OF WING SLOTS AND  
LEADING-EDGE SLATS ON THE LONGITUDINAL STABILITY  
CHARACTERISTICS OF A  $45^\circ$  SWEPTBACK  
WING-FUSELAGE CONFIGURATION

By Chris C. Critzos

## SUMMARY

An exploratory investigation to determine the effects of wing slots on the longitudinal stability characteristics of a  $45^\circ$  sweptback wing-fuselage combination was conducted in the Langley 16-foot transonic tunnel. The wing had NACA 65A006 airfoil sections, an aspect ratio of 4, taper ratio of 0.6, and incorporated various combinations of three outboard 35-percent-semispan wing slots exhausting on the wing upper surface at the 15-, 30-, and 70-percent-chord stations. Detached leading-edge slats of 35 percent semispan and  $0^\circ$  deflection and a 20-percent-chord trailing-edge extension were also tested in conjunction with the wing slots. Data were obtained at angles of attack from  $0^\circ$  to  $20^\circ$  and at Mach numbers from 0.80 to 0.94 and data at low angles of attack were obtained for Mach numbers up to 1.05. The Reynolds number varied from  $5.4 \times 10^6$  to  $7.6 \times 10^6$ .

Only small improvements in longitudinal stability resulted from the use of wing slots alone. The use of the detached leading-edge slats in conjunction with the wing slots was required for significantly beneficial results throughout the Mach number range investigated where longitudinal instability occurred.

## INTRODUCTION

The use of swept wings of moderate aspect ratio in the design of present-day fighter-type airplanes has emphasized the importance of the longitudinal stability problems encountered by such wings at subsonic and transonic speeds. At subsonic speeds the pitch-up tendency of thin swept wings is the result of leading-edge vortex-type flow and consequent

CONFIDENTIAL

UNCLASSIFIED

separation of the flow over the outboard portion of the wing (ref. 1). This subsonic instability has been greatly alleviated for particular swept wings by the addition of fences and leading-edge devices such as chord-extensions and slats (refs. 2 and 3). At transonic speeds the longitudinal instability of swept wings is the result of shock-induced flow separation in the region of the wing tip. The arrangements of fences, chord-extensions, and leading-edge slats, which were successful in alleviating the subsonic longitudinal instability of swept wings, were only slightly effective in eliminating the pitch-up problem in the transonic speed range, particularly for Mach numbers between 0.94 and 0.96. However, inasmuch as undrooped leading-edge slats indicated a slight superiority over chord-extensions as a wing auxiliary control device in the transonic range (compare results of refs. 2 and 3), it was believed that additional boundary-layer scavenging in the outboard portion of the wing would further alleviate the stability problem in this range. The present investigation was therefore planned to explore the use of spanwise wing slots and other outer panel devices on a swept wing which had been investigated for longitudinal stability improvements with other previously developed devices.

The 45° sweptback wing used for the present investigation had an aspect ratio of 4, a taper ratio of 0.6, and NACA 65A006 airfoil sections parallel to the plane of symmetry. The basic data for this wing were previously reported in reference 4. The effects of chord-extensions, leading-edge slats, and fences on the same wing were reported in references 2, 3, 5, and 6. The longitudinal stability characteristics of the slotted wing were obtained in the Langley 16-foot transonic tunnel for several combinations of three outboard, 35-percent-semispan slots for a wing-body combination equipped with a vertical tail. The three wing slots opened on the upper surface of the wing at about the 15-, 30-, and 70-percent-chord station. Horizontal tail-on data were also obtained for one slotted-wing configuration of the present study. The slotted wing was also investigated in combination with 35-percent-semispan leading-edge slats and floating trailing-edge extensions.

Because the present work was primarily concerned with longitudinal stability at high subsonic speeds, lift coefficients at least as high as 0.80 were investigated only at Mach numbers of 0.80, 0.90, and 0.94. Low angle-of-attack data were obtained for Mach numbers up to 1.05 to establish drag penalties. The test Reynolds number varied from about  $5.4 \times 10^6$  to  $7.6 \times 10^6$  based on the wing mean aerodynamic chord.

#### COEFFICIENTS AND SYMBOLS

- b wing span
- c local wing chord

$\bar{c}$	mean aerodynamic chord
$C_D$	drag coefficient, $\frac{\text{Drag}}{qS}$
$C_L$	lift coefficient, $\frac{\text{Lift}}{qS}$
$C_m$	pitching-moment coefficient about 0.25 $\bar{c}$ of wing, $\frac{\text{Pitching moment}}{qS\bar{c}}$
$D$	maximum diameter of fuselage, in.
$M$	free-stream Mach number
$P_b$	base pressure coefficient
$q$	free-stream dynamic pressure, $\frac{1}{2}\rho V^2$
$R$	Reynolds number, based on $\bar{c}$ of wing
$S$	total wing area
$V$	free-stream velocity
$\alpha$	angle of attack of fuselage center line relative to $V$
$\rho$	density of air

## APPARATUS

### Tunnel

The tests were conducted in the Langley 16-foot transonic tunnel, a single-return octagonal slotted-throat wind tunnel. A detailed description of this tunnel is presented in reference 7. As indicated in this reference, the maximum variation of the average Mach number along the test-section center line in the vicinity of the model is about  $\pm 0.002$ . Mach numbers in the present report are given to the nearest 0.01.

## Model Support System

A single swept-cantilever strut supported the sting-mounted model for the present tests. This support system, as described in detail in reference 4, held the model near the tunnel center line throughout the angle-of-attack range.

## MODELS

### Basic Model

The wing for the present investigation had an aspect ratio of 4, a taper ratio of 0.6,  $45^\circ$  sweep of the quarter-chord line, and NACA 65A006 airfoil sections parallel to the plane of symmetry.

Ordinates for the 6A-series airfoil sections may be found in reference 8. The wing was made of aluminum alloy and was designed to have no twist or incidence relative to the fuselage, and checks of the model indicated these objectives were achieved to within  $\pm 0.1^\circ$ . The wing was mounted in the midwing position on the fuselage.

The fuselage consisted of a cylindrical body of revolution with an ogival nose and a slightly boattailed afterbody. The fuselage for the present tests differed in length from that used in references 2 to 6, having a fineness ratio of 11 as compared with 10. The horizontal tail was geometrically similar to the wing and was mounted in the midfuselage position at an angle of incidence of  $-4^\circ$ . The ratio of the span of the horizontal tail to the span of the wing was 0.427. The vertical tail had an aspect ratio of 1.5 measured to the fuselage center line, a taper ratio of 0.3,  $45^\circ$  sweep at the quarter-chord line, and NACA 65A005 airfoil sections.

Both the vertical and horizontal tails were bolted to the fuselage and all gaps were filled and faired smooth. The dimensional details of the model are given in figure 1(a) and a photograph of the model mounted in the tunnel is given as figure 2(a).

### Wing Modifications

The basic wing was modified with various combinations of three tapered wing slots extending from the 0.65b/2 position to the 0.975b/2 position. The slots were numbered for reference starting with the slot nearest the leading edge of the wing. The center lines of the slots were located on the upper or exit surface at approximately 15.5, 30, and 70 percent of the chord; on the lower surface these center lines

were located at approximately 3.68, 15, and 55 percent of the chord. Pertinent dimensions for the slots are given in figure 1(b) and photographs of both surfaces of one wing showing the slotted area of the wing are given as figure 2(b). Modifications to slot 2 consisted of increasing the width of the slot opening on the wing lower surface from 0.014c to 0.017c by removing material from the forward slot face and of increasing the radius of the rounded portion of the slot on the wing upper surface. Details of these modifications are shown in figure 1(c).

The wing was also tested with leading-edge slats and with trailing-edge extensions. The slat configuration was formed by extending the segment of the wing ahead of slot 1 forward 9 percent of the chord and filling the original forward slot (slot 1) with a member whose forward face was identical with the undersurface of the slat. The slats, extending from the 65-percent-semispan position to the wing tip, had a chord of 14 percent of the wing chord and, unmodified, duplicated the undrooped 35-percent-semispan slats of reference 3. For the modified-slat configurations, the lip of the slot behind the leading-edge slat was rounded as shown in figure 1(c). The trailing-edge extensions consisted of free-floating flaps extending from the 65-percent-semispan position to the wing tip. The chord of these flaps was equal to 20 percent of the local wing chord. The flaps were supported with end bearings and were free to pivot on a hinge line which coincided with the original trailing edge of the wing. A filler was used on the wing to fair the upper and lower surfaces from the trailing-edge extension to a point of tangency on the wing at about the 60-percent-chord point. Dimensional details of the leading-edge slats and trailing-edge extensions are given in figure 1(d).

#### Wing-Body-Tail Combinations

Tail-off and tail-on notations in the figures and discussion of the present paper refer only to the horizontal-tail surfaces. The tail-off configurations were equipped with a vertical tail; for tail-on tests, the horizontal-tail was added to the tail-off configurations.

#### TESTS

The present investigation consisted of measuring the aerodynamic forces and moments for a range of Mach numbers from 0.80 to 1.05. Test points were taken at 2° increments from angles of attack of 0° to 20°, 16°, and 14° for Mach numbers of 0.80, 0.90, and 0.94, respectively, and to 4° only for the remaining Mach numbers. The forces and moments were measured by a six-component electrical strain-gage balance mounted within the fuselage.

The Reynolds number for the present tests, based on a wing mean aerodynamic chord of 1.531 feet, ranged from  $5.4 \times 10^6$  to  $7.6 \times 10^6$ . (See fig. 3.)

## CORRECTIONS AND PRECISION

### Force-Data Accuracy

The Mach numbers assigned to the data presented herein are accurate to within  $\pm 0.01$ . The data were not adjusted for sting-interference and wing aeroelastic effects. It has been established that boundary-interference effects are very small in this slotted wind tunnel, at least for Mach numbers as high as 1.03, and no attempt to correct the data for these effects has been made. The accuracy of the measured coefficients, based on balance accuracy and repeatability of data, is estimated to be within the following limits:

$C_L$ . . . . .	$\pm 0.01$
$C_D$ -	
At low lift coefficients . . . . .	$\pm 0.001$
At high lift coefficients . . . . .	$\pm 0.005$
$C_m$ . . . . .	$\pm 0.005$

### Base Pressure

By use of the base pressure as measured by three orifices located about 2 inches inside the base of the model, the lift and drag data were adjusted to the condition of free-stream static pressure at the base of the model. The base pressure coefficients for the tail-off and tail-on configurations are presented as functions of Mach number in figure 4. Based on repeatability of measurements, these coefficients are estimated to be accurate to within  $\pm 0.01$ .

### Angle of Attack

The model attitude was measured by a pendulum-type strain-gage inclinometer. An adjustment for airstream misalignment ( $0.30^\circ$  upflow angle) was made, and the angles of attack reported herein are estimated to be accurate to within  $\pm 0.1^\circ$ .

## RESULTS AND DISCUSSION

The results of tests of slotted-wing configurations on a  $45^\circ$  swept-back wing-body configuration in the Langley 16-foot transonic tunnel are presented in figures 5 to 9.

The selection of the best slotted-wing configuration is based on the comparison of data for various slot configurations shown in figure 5. Data for the best slotted-wing configuration of the present tests are compared with the basic model data in figure 6. The best leading-edge slat slotted-wing configuration is compared with the best slotted-wing configuration in figure 7. Data for several modifications to improve the former configuration are shown in figure 8. Tail-on data are compared for the basic model and the best leading-edge slat slotted-wing configuration with and without a trailing-edge extension in figure 9.

The variations in lift, drag, and pitching-moment coefficients with angle of attack and lift coefficient for the various configurations are shown for Mach numbers from 0.80 to 1.05. Data were obtained for the full angle-of-attack range only at a few representative Mach numbers where longitudinal instability was most severe ( $M = 0.80, 0.90, \text{ and } 0.94$ ). Data were obtained at low angles of attack for a wider Mach number range, however, to establish drag penalties.

## Pitching-Moment Characteristics

Effect of wing slots, tail off.- The pitching-moment-coefficient data shown in figure 5(a) indicate only slight improvements in the longitudinal stability of the basic model resulting from slotting the wing. Although the unstable break in the pitching-moment curves was not eliminated, the curves for the slotted-wing configurations were slightly more linear than those for the basic wing. The data also indicate the configuration with slots 1 and 2 open as being the most favorable. For this configuration, the unstable break in the pitching-moment curve was generally the least abrupt and the lift coefficient for this break was extended from 0.63 to 0.72 at a Mach number of 0.94. Data for this configuration are compared with the data for the basic model in figure 6.

Effect of leading-edge slats, tail off.- The addition of leading-edge slats to the slotted wing showed very little improvement in delaying the unstable break in the pitching-moment curve of the slotted-wing model to higher lift values (fig. 7(a)), although the break at all Mach numbers was less severe. Data for several modifications to the slotted-wing model equipped with leading-edge slats shown in figure 8(a) indicate only minor changes in the pitching-moment characteristics. Widening the entrance opening of slot 2 resulted in somewhat more negative pitching moments at



moderate lift values for Mach numbers of 0.90 and 0.94. The effects of altering the lip of the slot behind the leading-edge slat were negligible (fig. 8). Data are not presented for the slat configuration with both slots 2 and 3 open which indicated little or no change in the longitudinal stability characteristics.

Effect of free-floating trailing-edge extension, tail on.- It should be pointed out, at this point, that the results indicated by the addition of the trailing-edge extensions shown in figure 9 are not conclusive because of structural failure of these devices at an undetermined point in the investigation. For a Mach number of 0.80 there was no change in the pitching-moment characteristics due to the trailing-edge extensions (fig. 9(a)). For Mach numbers of 0.90 and 0.94, however, the linearity of the pitching-moment curves was improved. Due to the structural failure of this device, it is not known whether these improvements in linearity were due to the trailing-edge extension or to a delay in tip separation resulting from the thickened trailing edge of the wing.

#### Lift and Drag Characteristics

The lift-coefficient values for the various slotted-wing configurations shown in figure 5(b) indicate only minor changes in the lift characteristics of the basic model. The increase in drag coefficient at low lift coefficients, resulting from slotting the wing was also small, approaching about 0.003 at the higher Mach numbers (fig. 5(c)). Adding the leading-edge slats to the slotted wing indicated generally very little change in lift for moderate angles of attack and a gain in lift at high angles of attack (fig. 7(b)). Figure 7(c) indicates the drag for this configuration to be somewhat less than that for the slotted wing for lift coefficients above about 0.4.

The addition of the trailing-edge extensions generally indicated only minor changes in lift throughout the test range (fig. 9(b)). At low lift coefficients the drag was increased by about 0.002 to 0.004 for Mach numbers up to 0.94 (fig. 9(c)).

#### CONCLUDING REMARKS

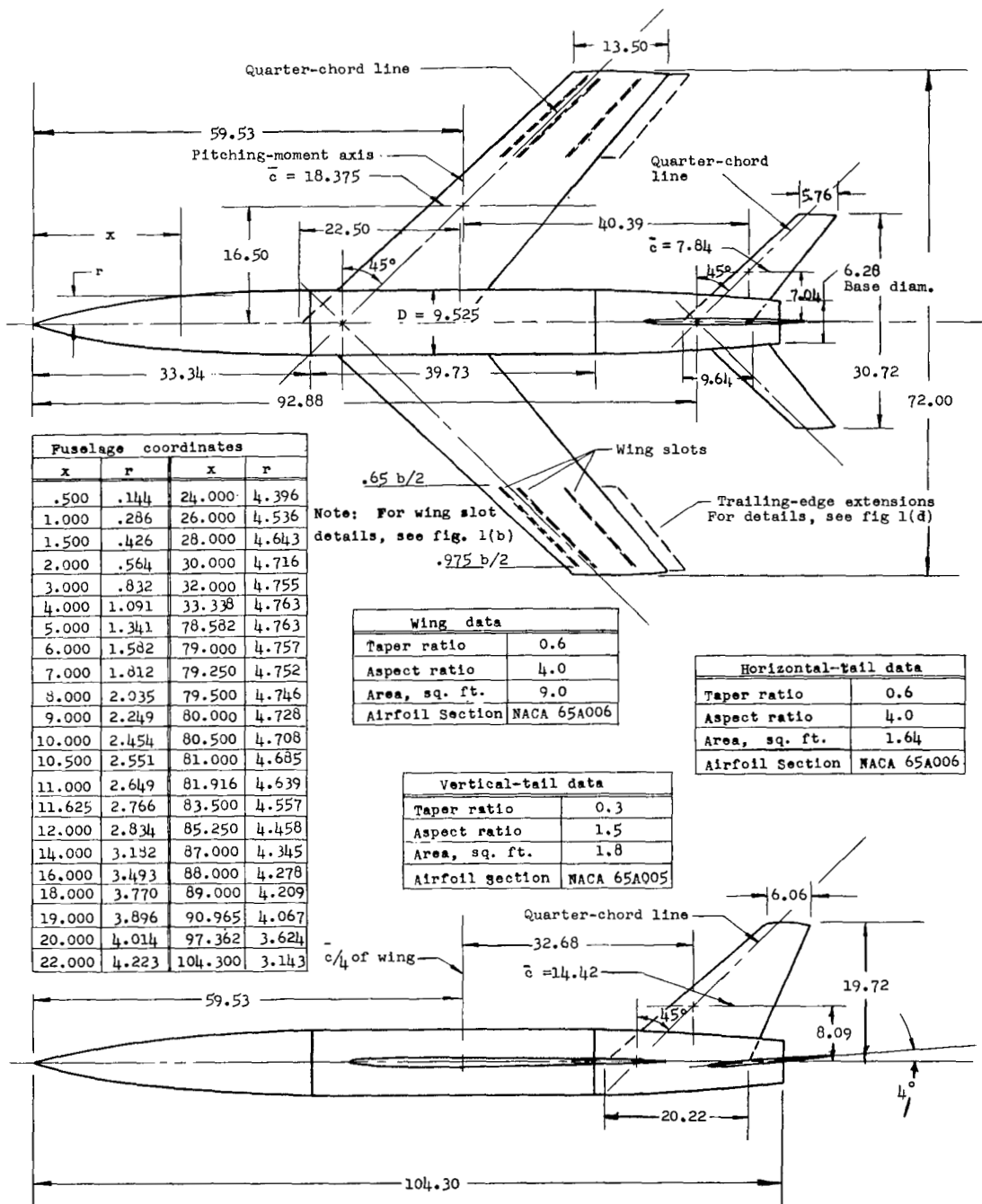
An exploratory investigation was made in the Langley 16-foot transonic tunnel of a  $45^\circ$  sweptback wing-fuselage combination equipped with outboard wing slots and leading-edge slats of 35 percent semispan to improve pitching-moment linearity in the high subsonic region. Only small improvements in longitudinal stability characteristics resulted from the use of wing slots alone. The use of detached leading-edge

slats in conjunction with the wing slots was required for significant beneficial results throughout the Mach number range investigated.

Langley Aeronautical Laboratory,  
National Advisory Committee for Aeronautics,  
Langley Field, Va., November 19, 1956.

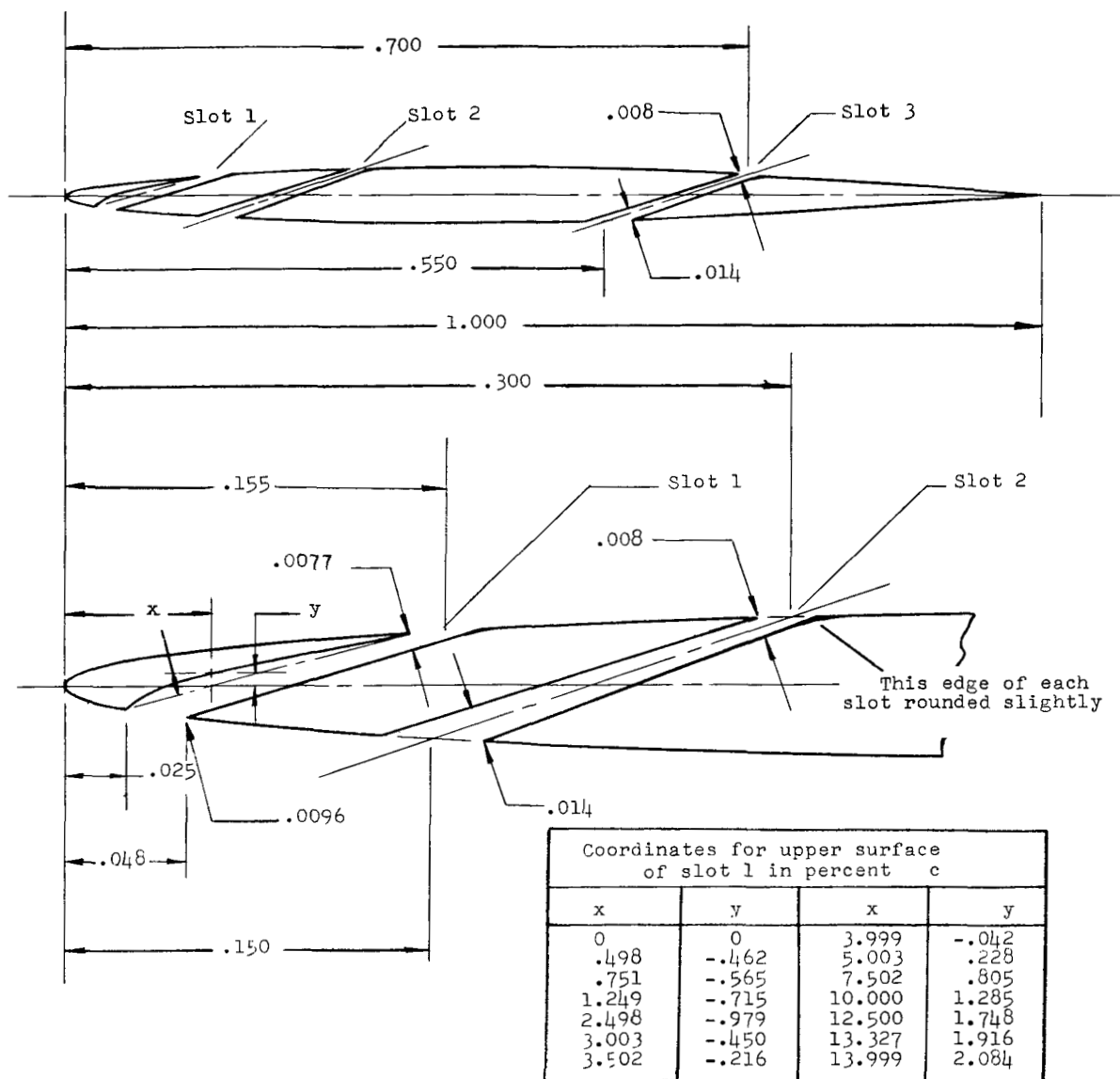
## REFERENCES

1. Lange, Roy H., Whittle, Edward F., Jr., and Fink, Marvin P.: Investigation at Large Scale of the Pressure Distribution and Flow Phenomena Over a Wing With the Leading Edge Swept Back  $47.5^\circ$  Having Circular-Arc Airfoil Sections and Equipped With Drooped Nose and Plan Flaps. NACA RM L9G15, 1949.
2. West, F. E., Jr., Liner, George, and Martz, Gladys S.: Effect of Leading-Edge Chord-Extensions on the Aerodynamic Characteristics of a  $45^\circ$  Sweptback Wing-Fuselage Combination at Mach Numbers of 0.40 to 1.03. NACA RM L53B02, 1953.
3. Runckel, Jack F., and Steinberg, Seymour: Effects of Leading-Edge Slats on the Aerodynamic Characteristics of a  $45^\circ$  Sweptback Wing-Fuselage Configuration at Mach Numbers of 0.4 to 1.03. NACA RM L53F23, 1953.
4. Hallissy, Joseph M., and Bowman, Donald R.: Transonic Characteristics of a  $45^\circ$  Sweptback Wing-Fuselage Combination - Effect of Longitudinal Wing Position and Division of Wing and Fuselage Forces and Moments. NACA RM L52K04, 1953.
5. West, F. E., Jr., and Henderson, James H.: Relationship of Flow Over a  $45^\circ$  Sweptback Wing With and Without Leading-Edge Chord-Extensions to Longitudinal Stability Characteristics at Mach Numbers From 0.60 to 1.03. NACA RM L53H18b, 1953.
6. Hieser, Gerald: An Investigation at Transonic Speeds of the Effects of Fences, Drooped Nose, and Vortex Generators on the Aerodynamic Characteristics of a Wing-Fuselage Combination Having a 6-Percent-Thick,  $45^\circ$  Sweptback Wing. NACA RM L53B04, 1953.
7. Ward, Vernon G., Whitcomb, Charles F., and Pearson, Merwin D.: Air-Flow and Power Characteristics of the Langley 16-Foot Transonic Tunnel With Slotted Test Section. NACA RM L52E01, 1952.
8. Loftin, Lawrence K., Jr.: Theoretical and Experimental Data for a Number of NACA 6A-Series Airfoil Sections. NACA Rep. 903, 1948. (Supersedes NACA TN 1368.)



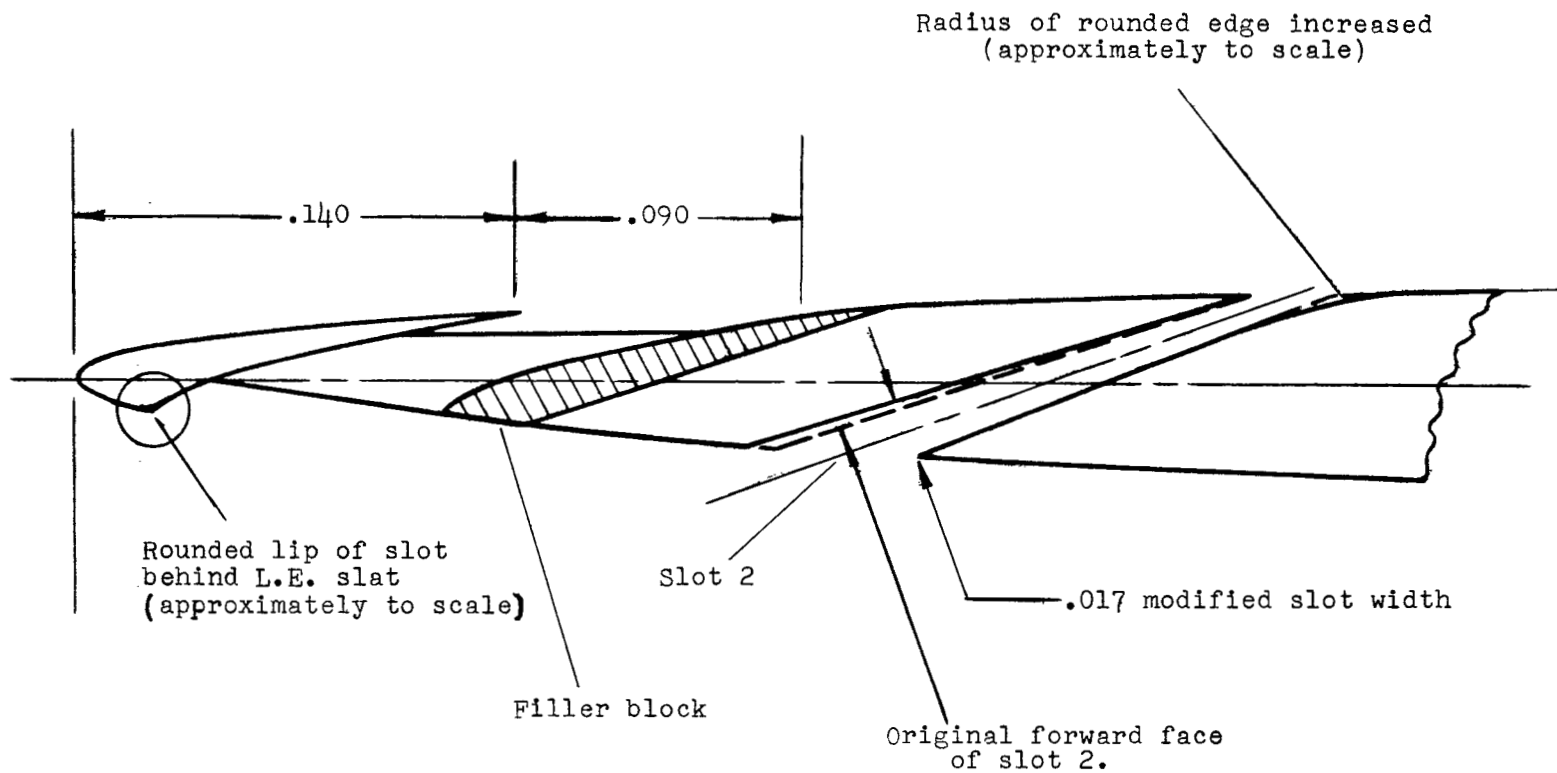
(a) Details of slotted wing-fuselage-tail combination. All dimensions given in inches unless otherwise noted.

Figure 1.- Dimensional details of slotted-wing model, leading-edge slats, and trailing-edge extensions.



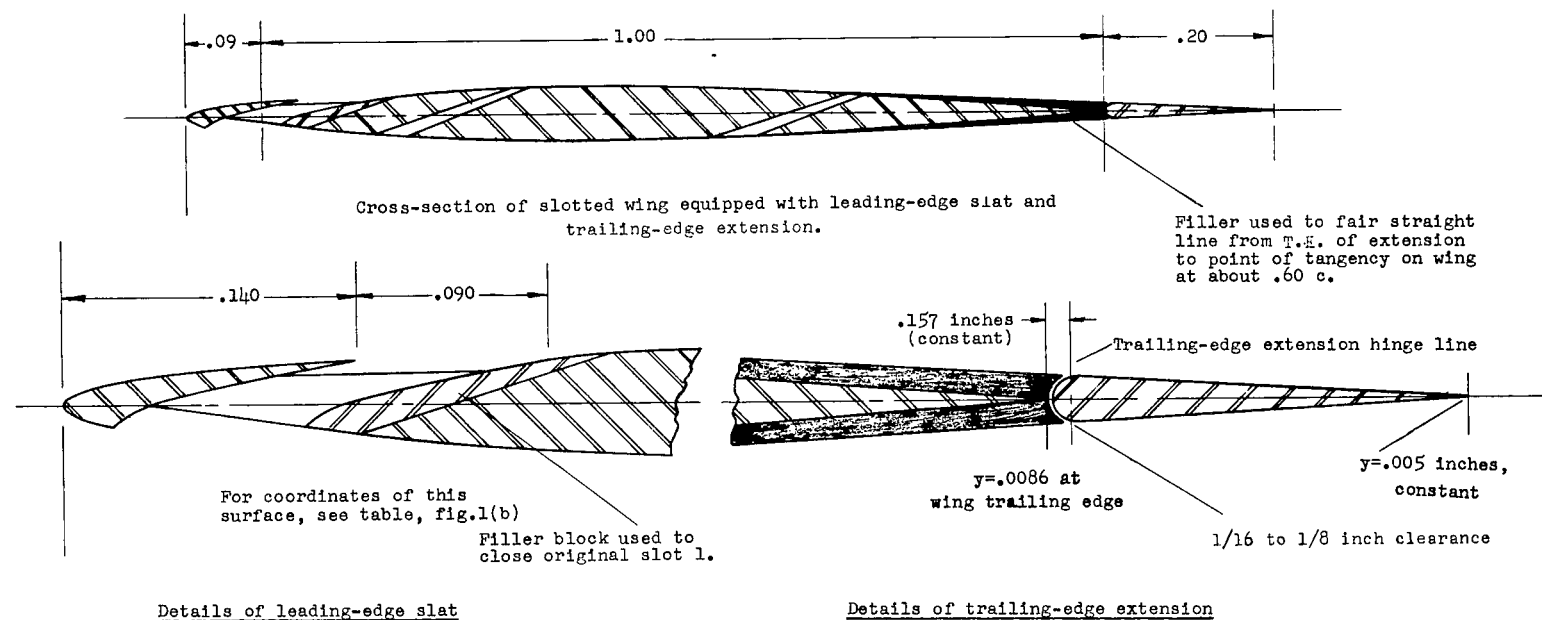
(b) Details of slotted wing. All dimensions given as a ratio of local chord.

Figure 1.- Continued.



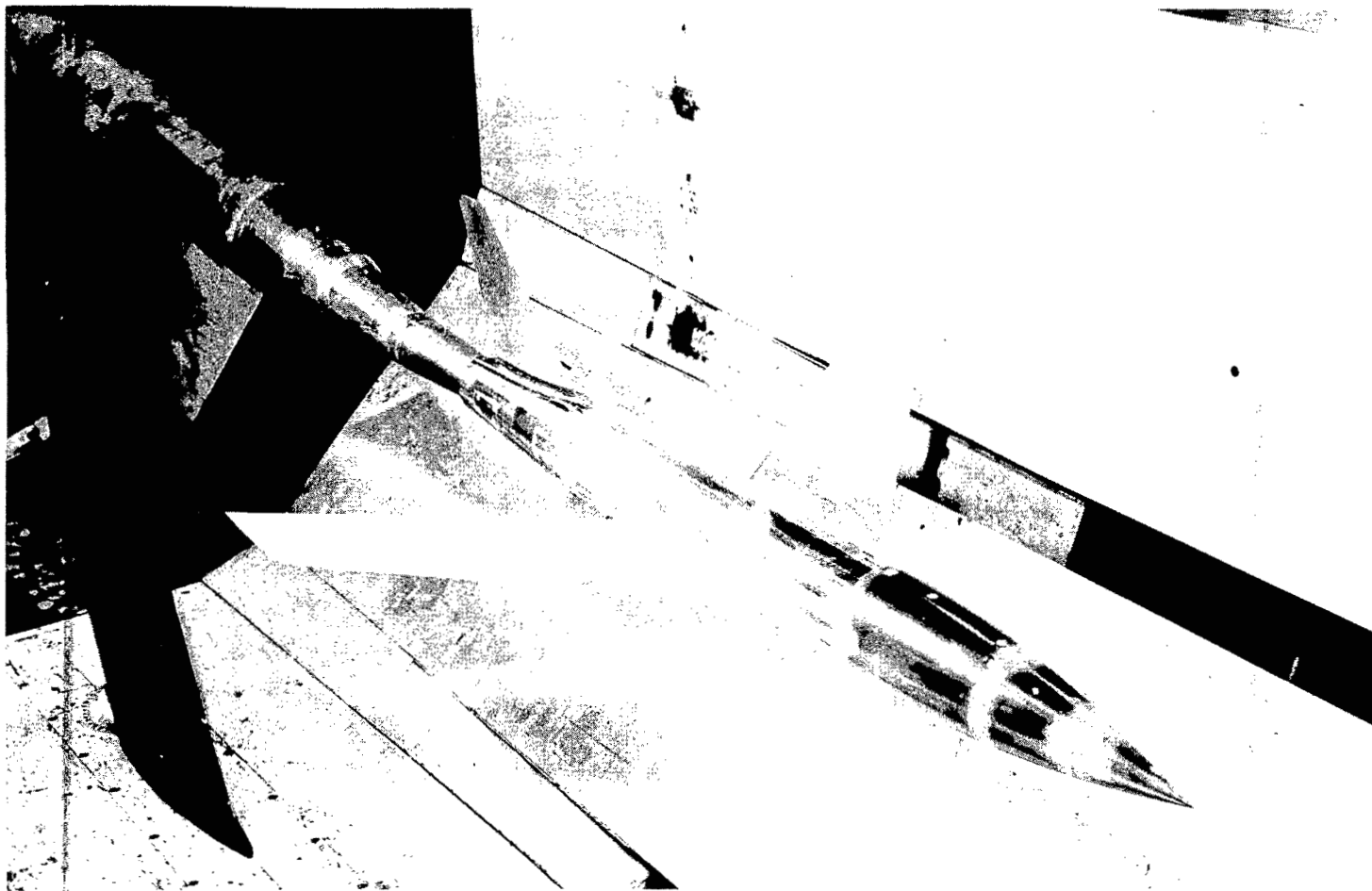
(c) Details of modifications to lip of slot behind leading-edge slat and to slot 2.  
All dimensions given as a ratio of local chord.

Figure 1.- Continued.



(d) Details of leading-edge slats and trailing-edge extensions. All dimensions given as a ratio of local chord unless otherwise noted.

Figure 1.- Concluded.



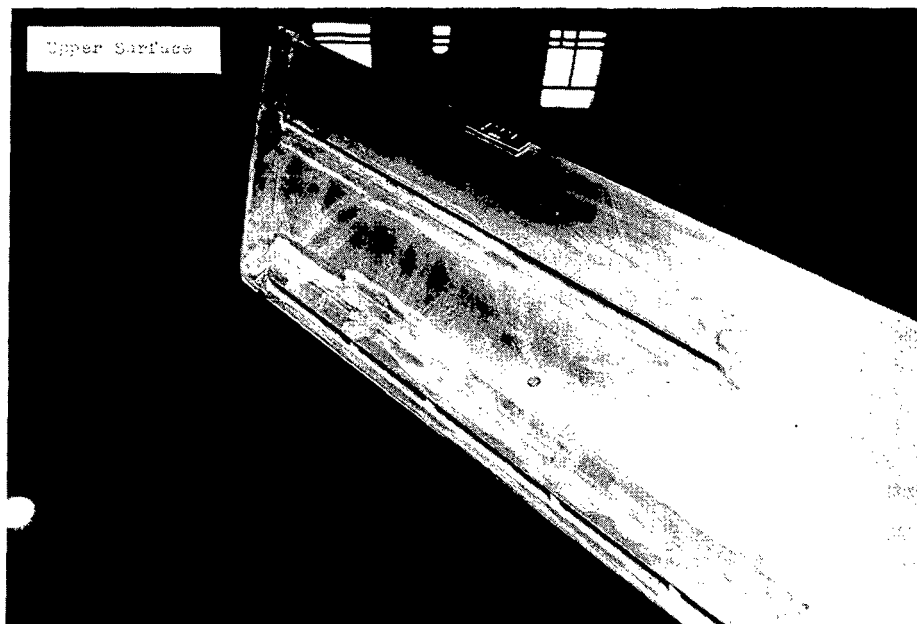
L-88797  
(a) Wing-fuselage configuration shown with vertical tail in Langley 16-foot transonic tunnel.

Figure 2.- Photographs of model.





L-88796.1



(b) Slotted-wing details.

L-88795.1

Figure 2.- Concluded.

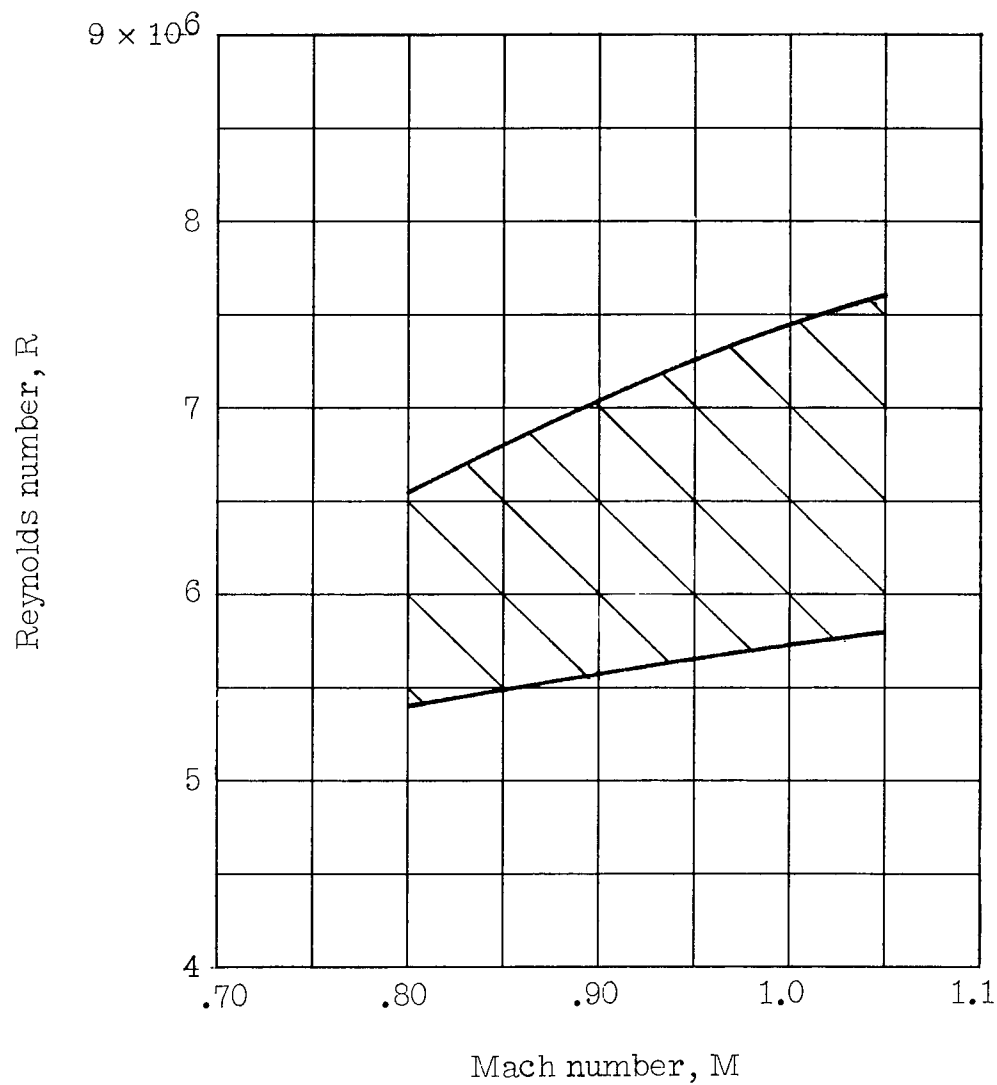


Figure 3.- Variation of Reynolds number (based on wing mean aerodynamic chord) with Mach number in the Langley 16-foot transonic tunnel.

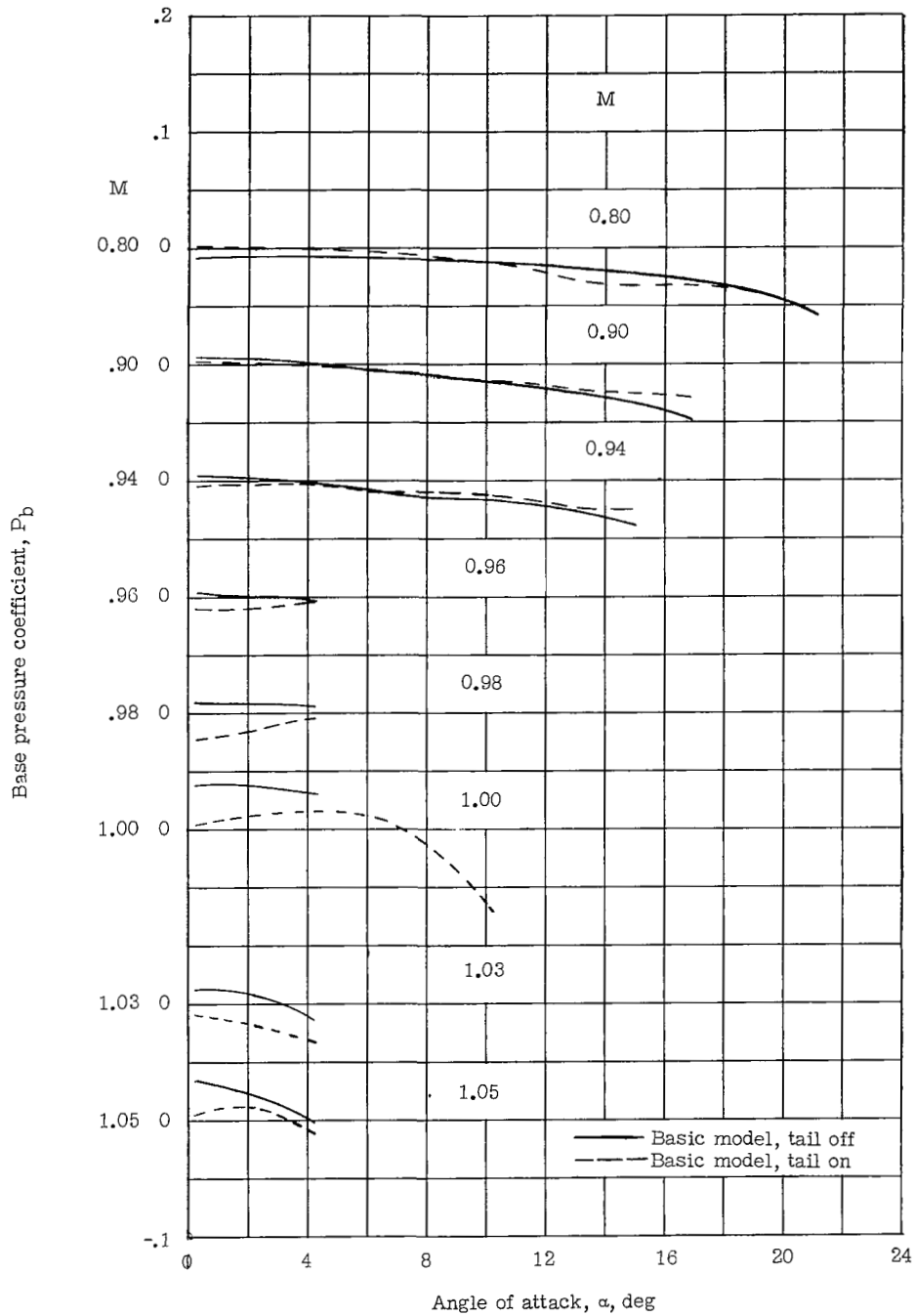
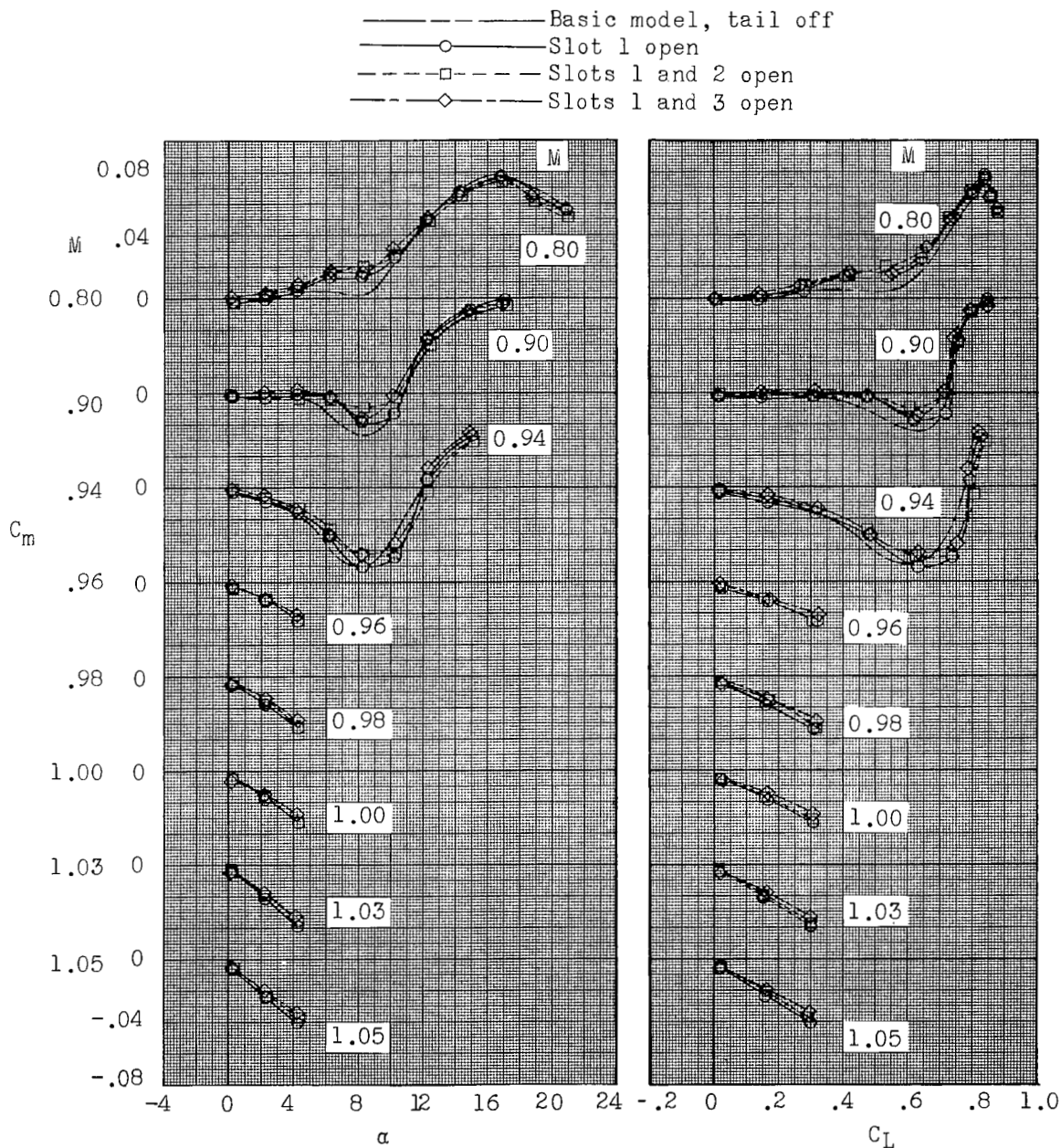
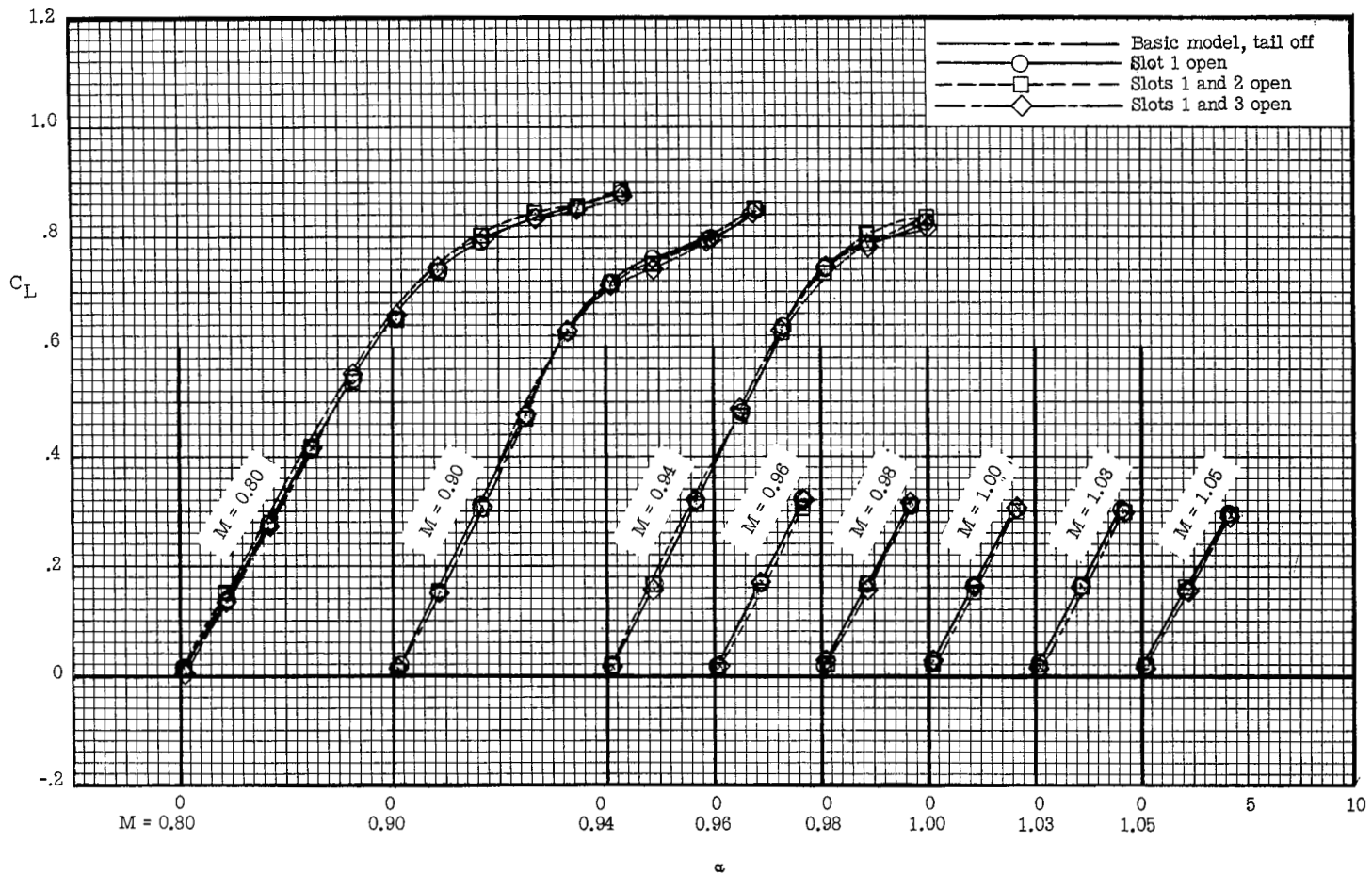


Figure 4.- Variation of base pressure coefficient with angle of attack of the basic tail-off and tail-on configurations at various Mach numbers in the Langley 16-foot transonic tunnel.



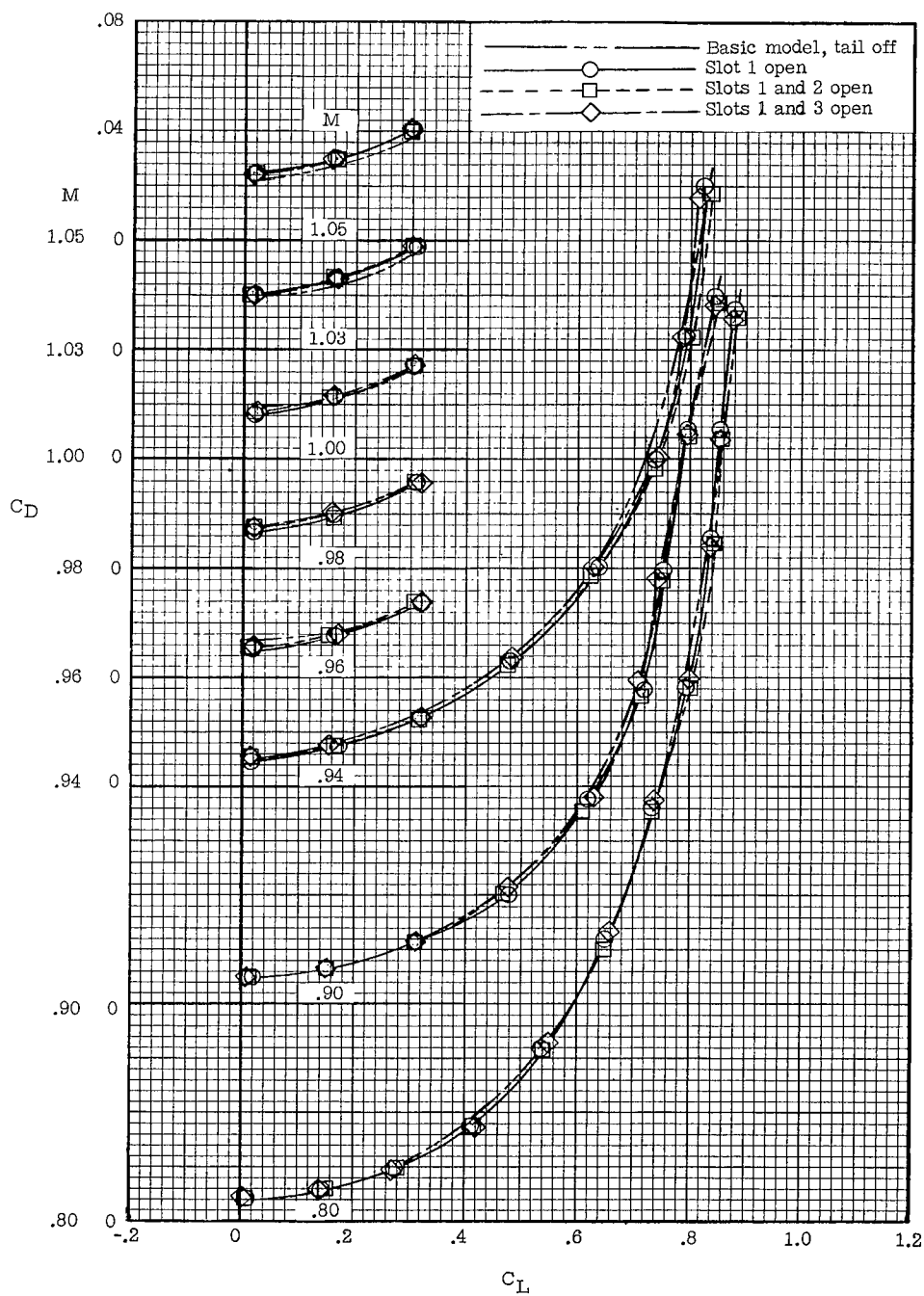
(a)  $C_m$  plotted against  $\alpha$  and  $C_m$  plotted against  $C_L$ .

Figure 5.- Effects of several combinations of wing slots on the longitudinal aerodynamic characteristics of the basic tail-off configuration.



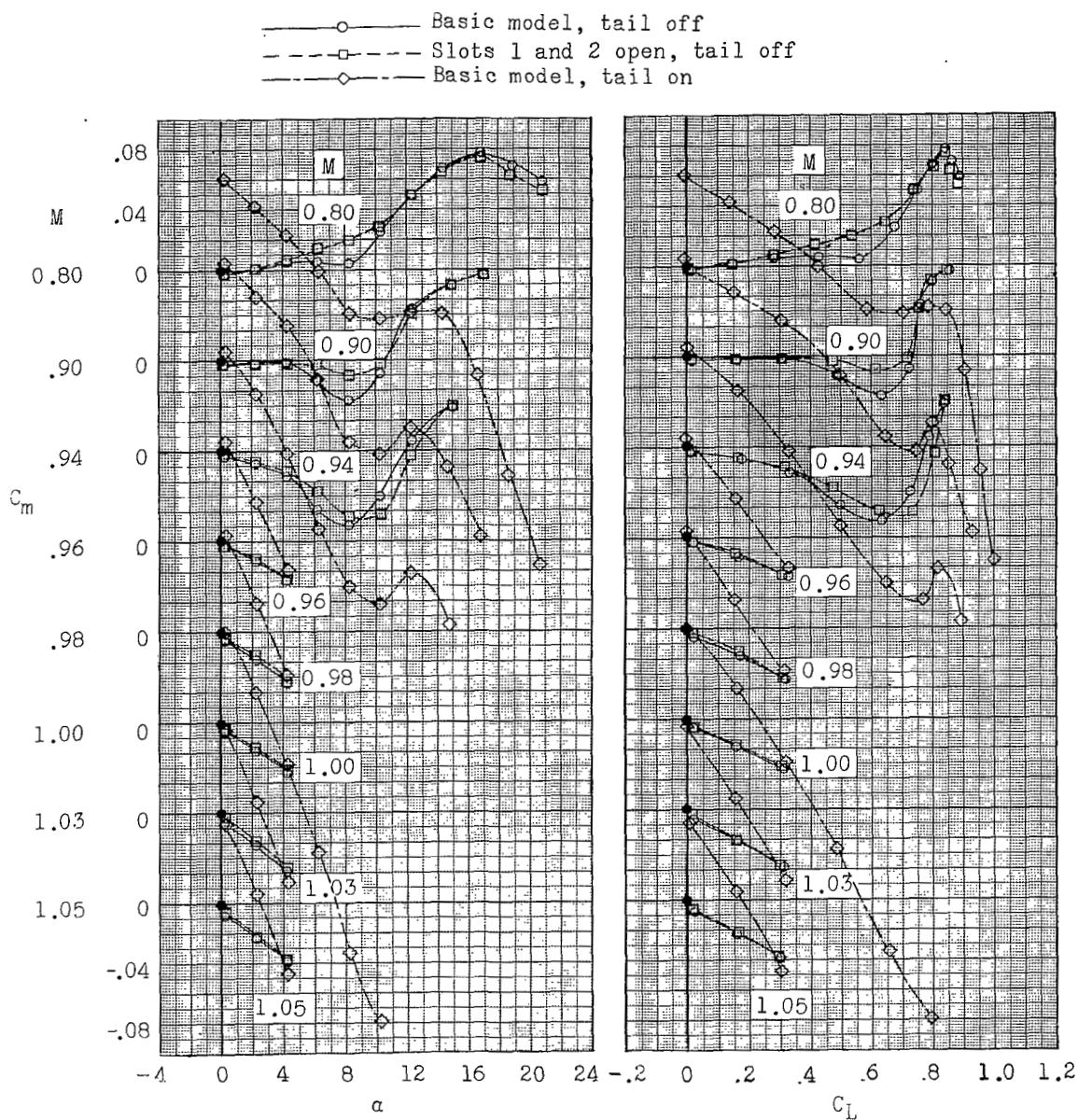
(b)  $C_L$  plotted against  $\alpha$ .

Figure 5.- Continued.



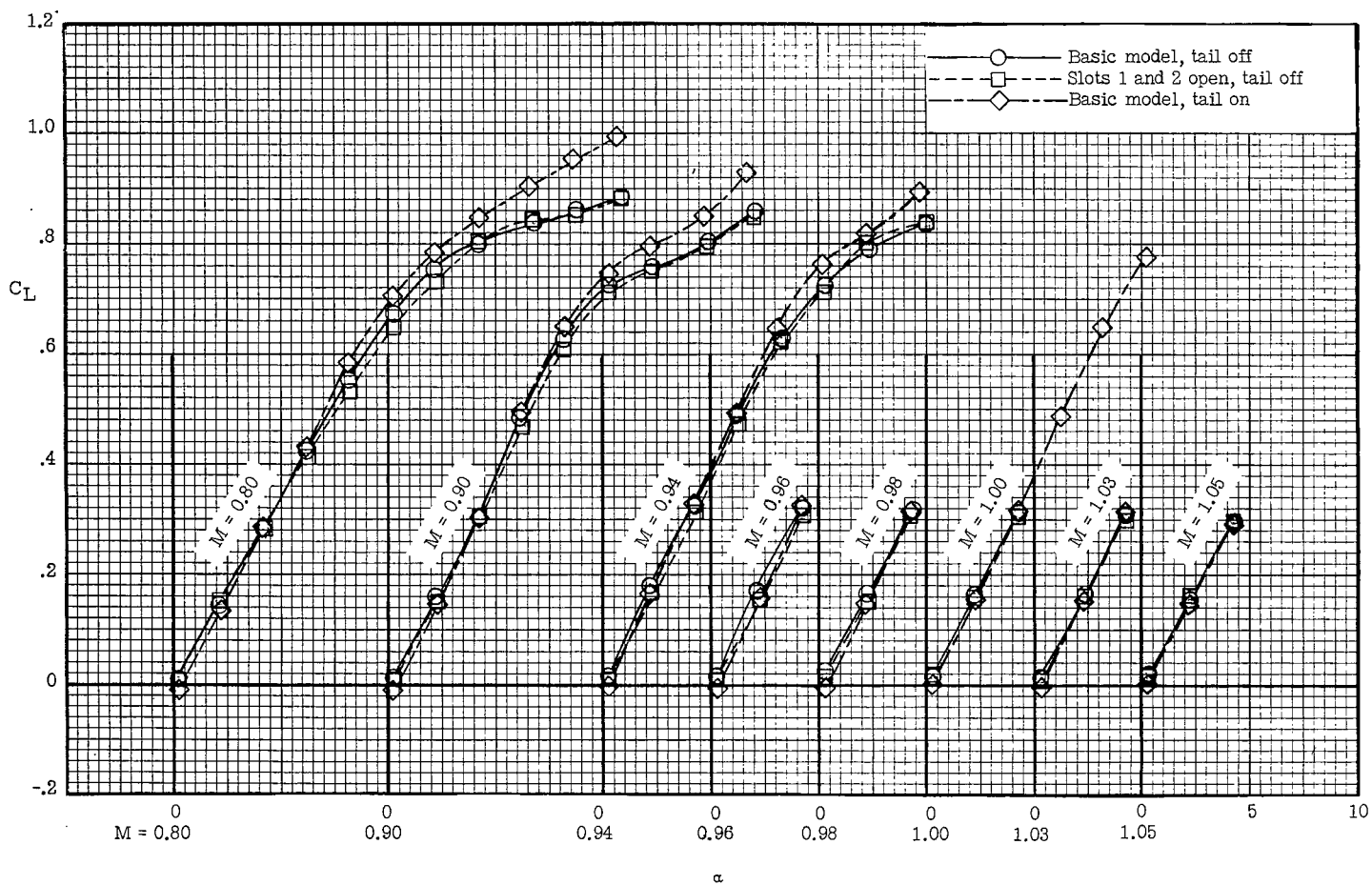
(c)  $C_D$  plotted against  $C_L$ .

Figure 5.- Concluded.



(a)  $C_m$  plotted against  $\alpha$  and  $C_m$  plotted against  $C_L$ .

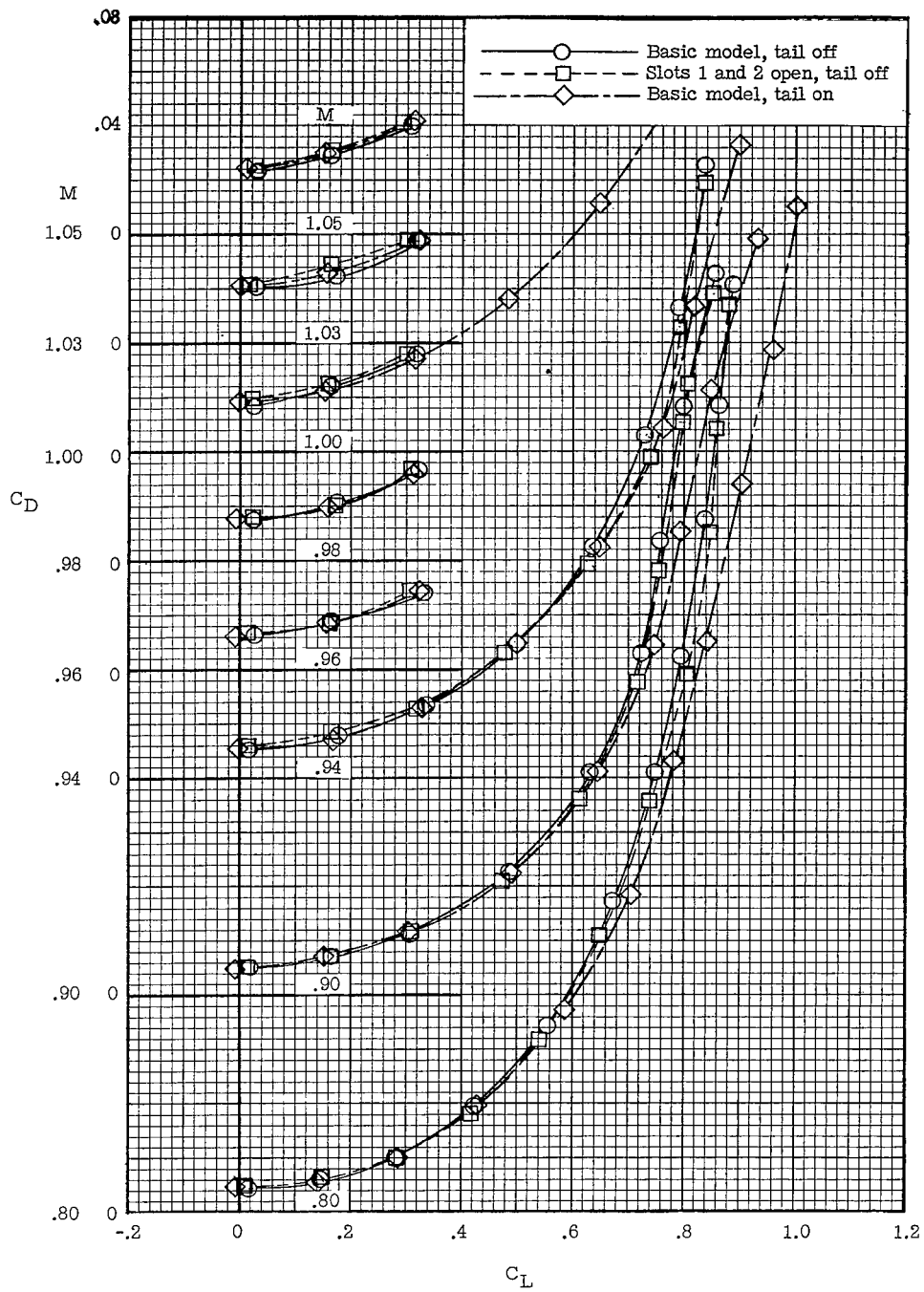
Figure 6.- Comparison of the longitudinal aerodynamic characteristics of the basic tail-off configuration with the basic tail-on configuration and with the slotted-wing tail-off configuration having slots 1 and 2 open.



(b)  $C_L$  plotted against  $\alpha$ .

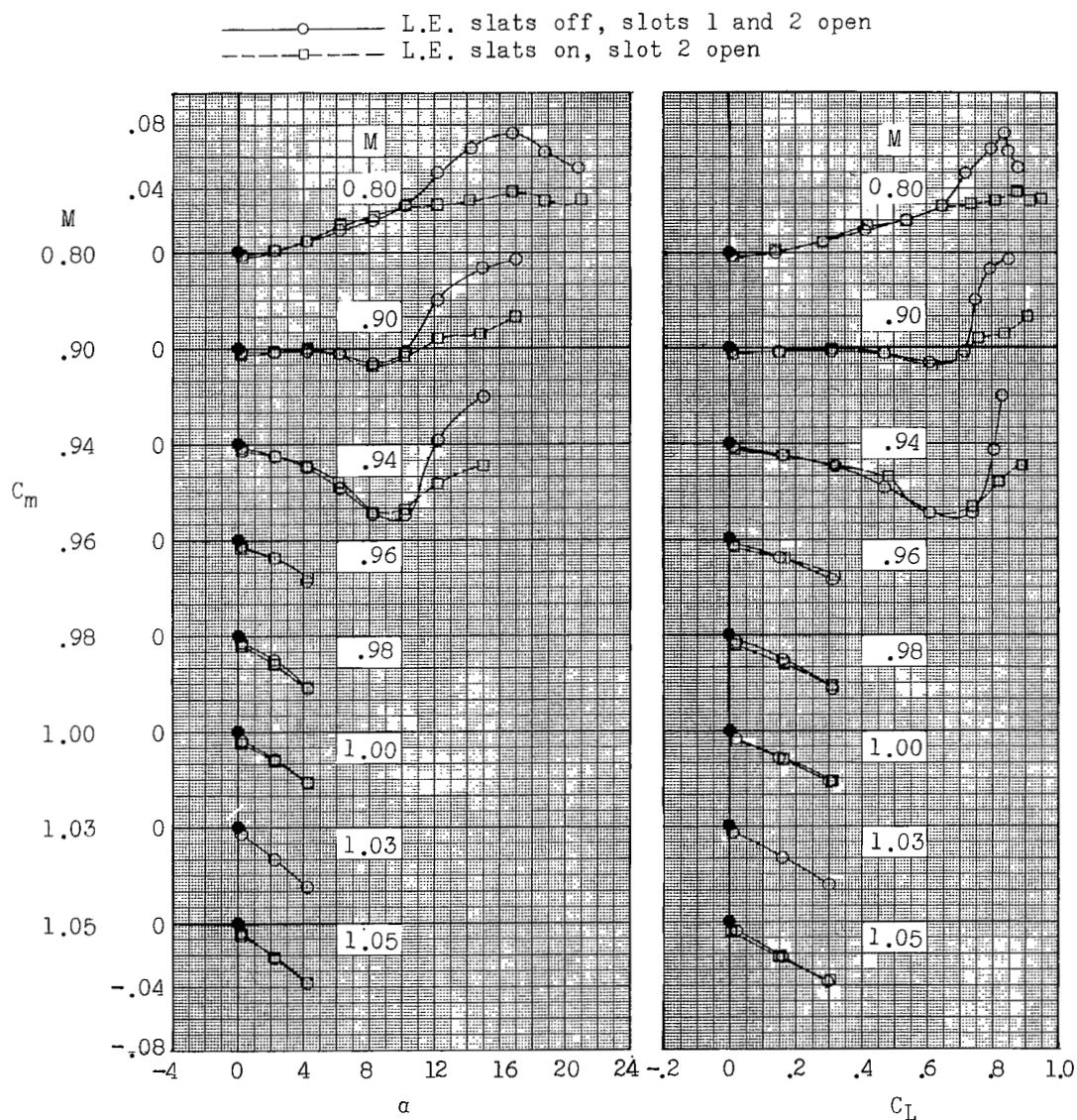
Figure 6.- Continued.





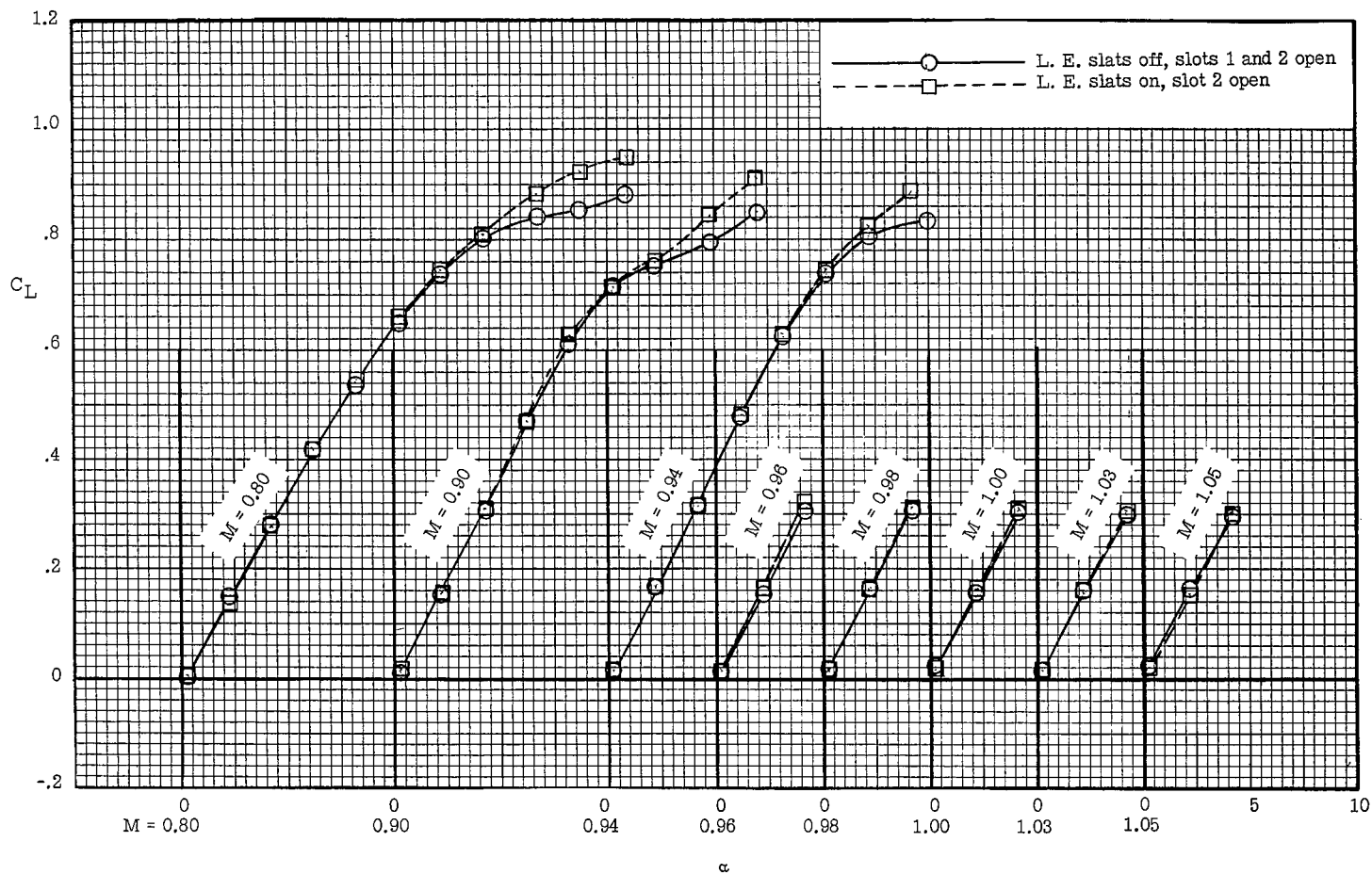
(c)  $C_D$  plotted against  $C_L$ .

Figure 6.- Concluded.



(a)  $C_m$  plotted against  $\alpha$  and  $C_m$  plotted against  $C_L$ .

Figure 7.- Effects of adding leading-edge slats and closing slot 1 on the longitudinal aerodynamic characteristics of the slotted-wing tail-off configuration having wing slots 1 and 2 open.



(b)  $C_L$  plotted against  $\alpha$ .

Figure 7.- Continued.

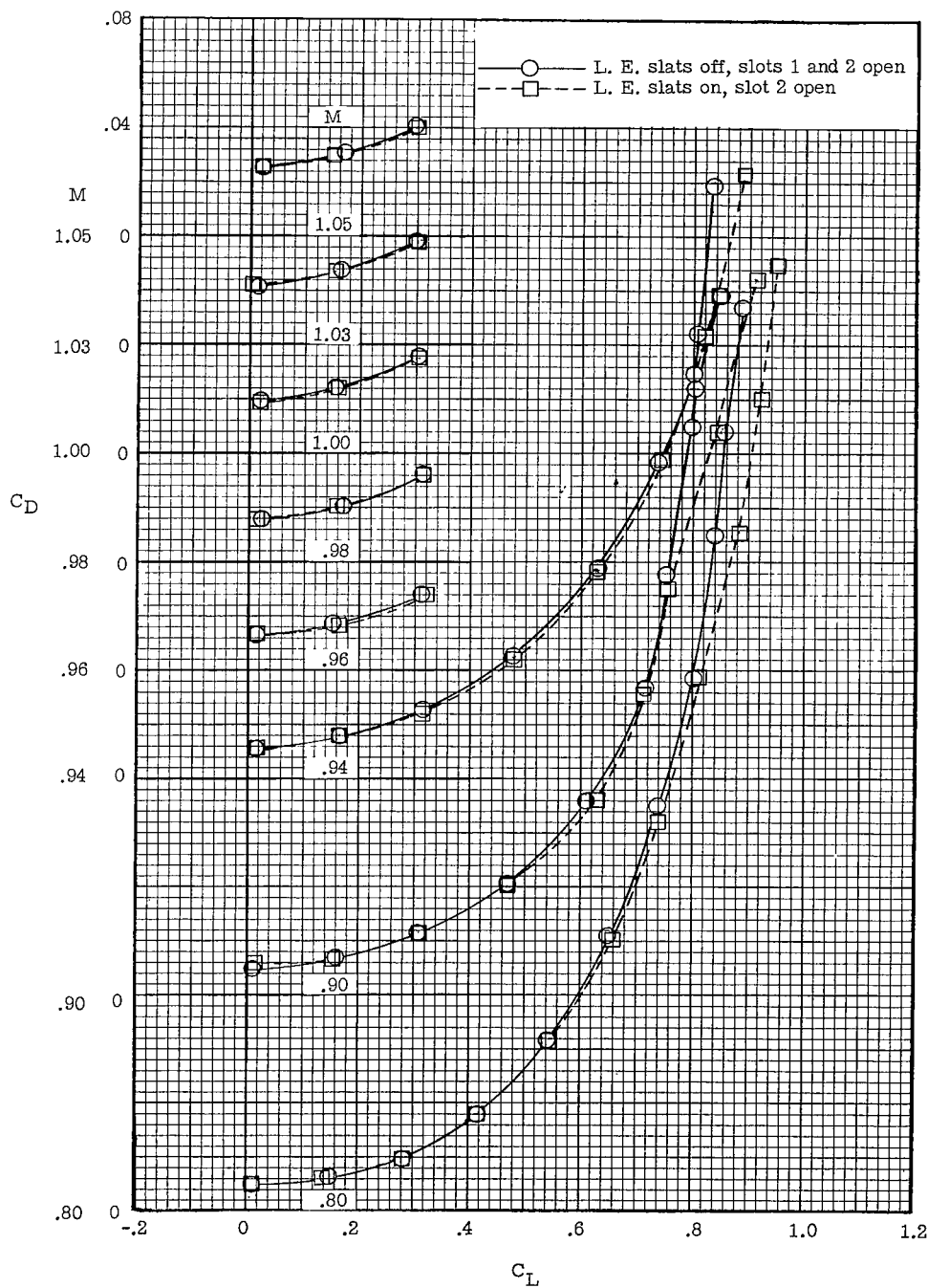
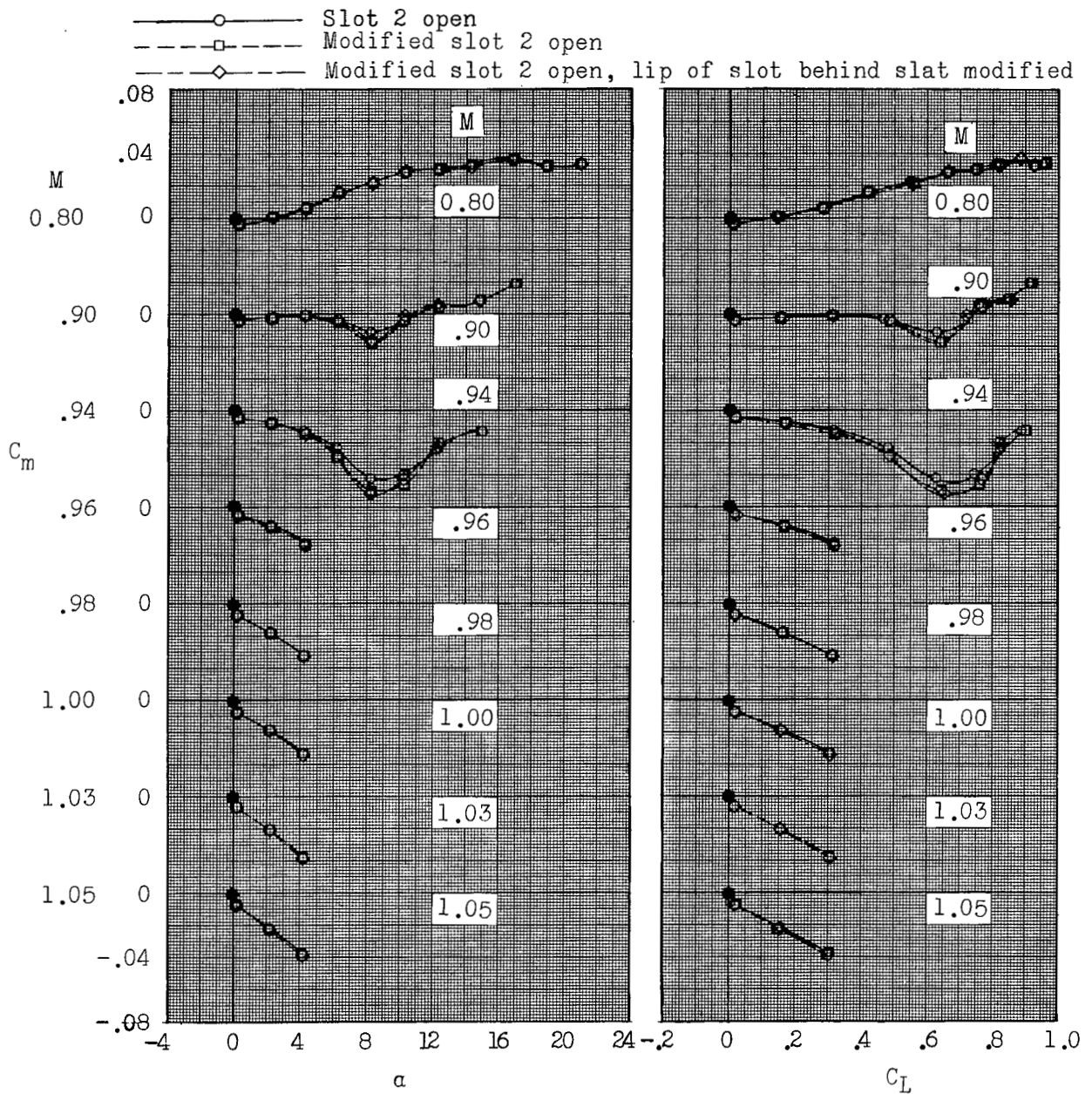
(c)  $C_D$  plotted against  $C_L$ .

Figure 7.- Concluded.



(a)  $C_m$  plotted against  $\alpha$  and  $C_m$  plotted against  $C_L$ .

Figure 8.- Effects of modifications to wing slot 2 and to the lip of the slot behind the leading-edge slats on the longitudinal aerodynamic characteristics of the slotted-wing leading-edge slat configuration. Tail off.

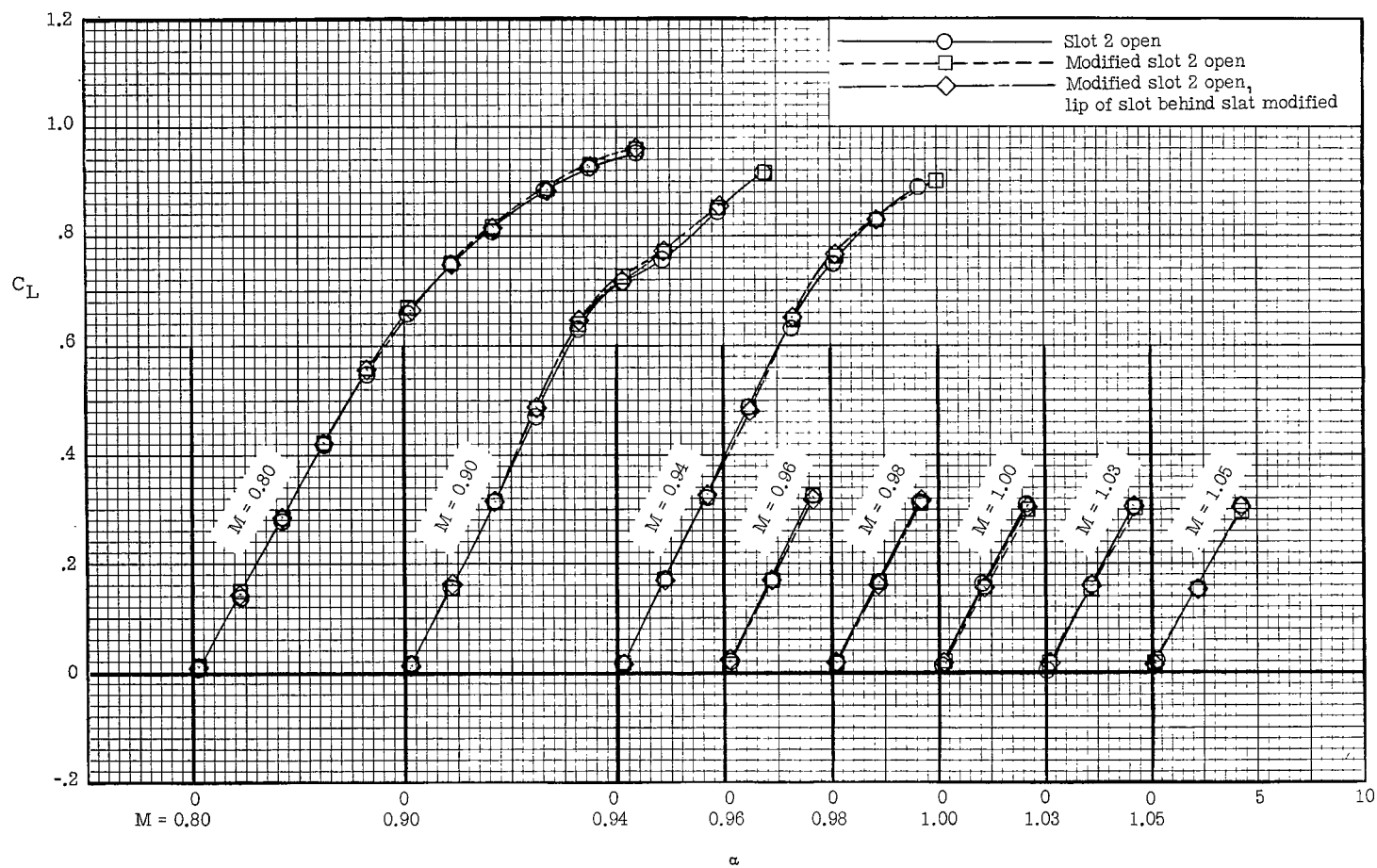
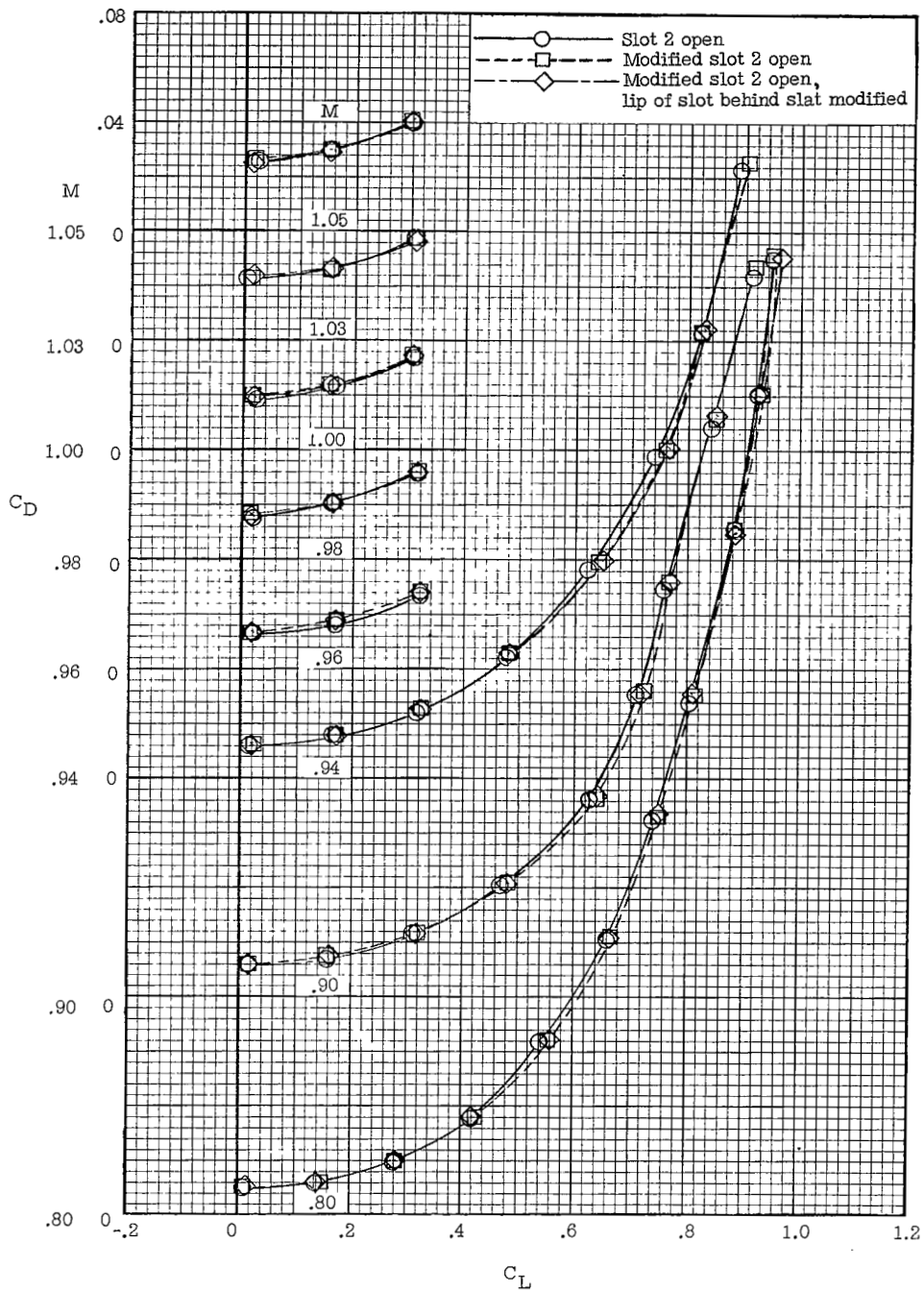
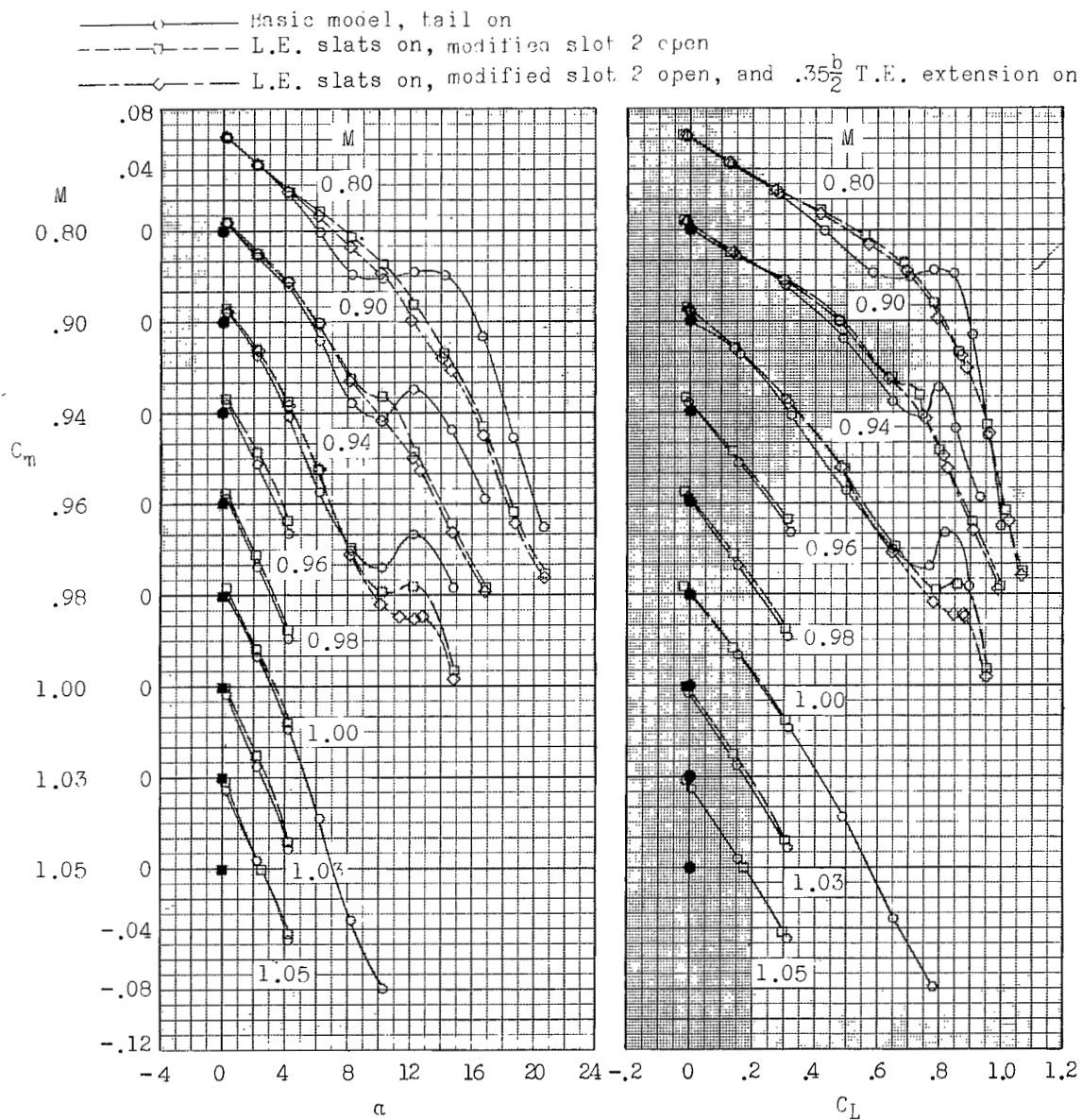
(b)  $C_L$  plotted against  $\alpha$ .

Figure 8.- Continued.



(c)  $C_D$  plotted against  $C_L$ .

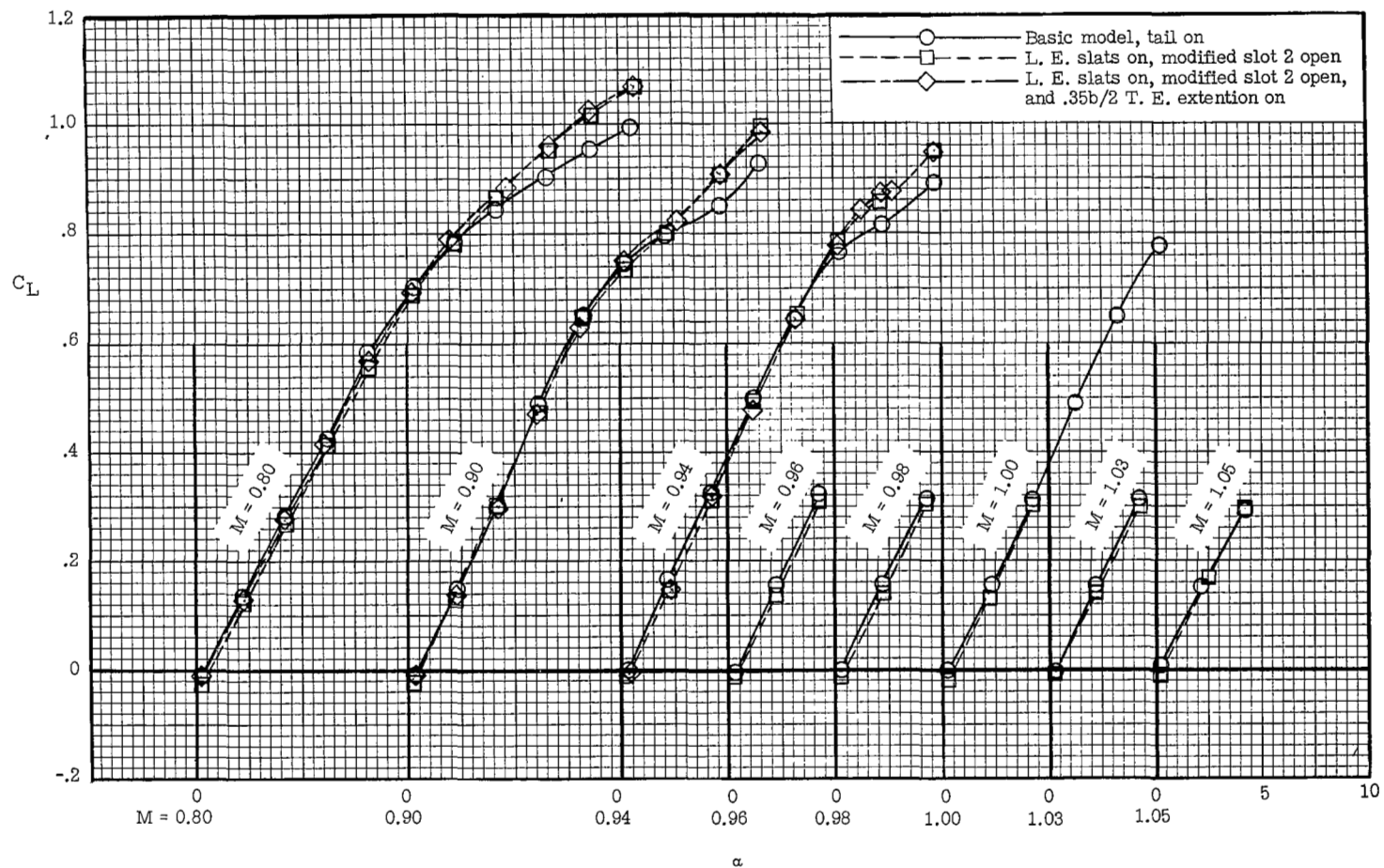
Figure 8.- Concluded.



(a)  $C_m$  plotted against  $\alpha$  and  $C_m$  plotted against  $C_L$ .

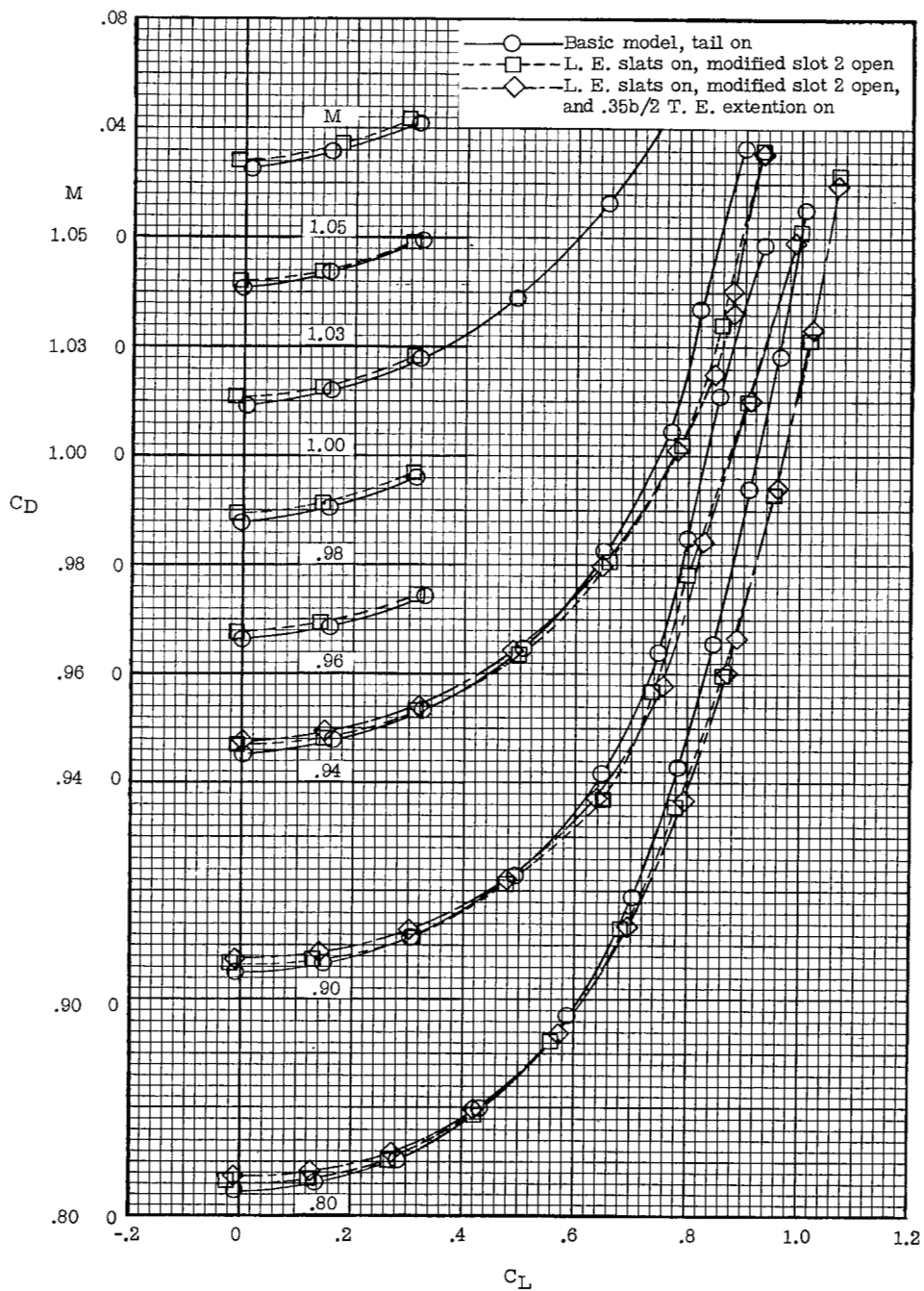
Figure 9.- Comparison of the longitudinal aerodynamic characteristics of the basic tail-on configuration with the best slotted-wing leading-edge-slat combination with and without the trailing-edge extension.





(b)  $C_L$  plotted against  $\alpha$ .

Figure 9.- Continued.



(c)  $C_D$  plotted against  $C_L$ .

Figure 9.- Concluded.

NASA Technical Library



3 1176 01437 7270



9 4 4

9 4 4

